

Fig. 1 a A cross-sectional image of the fovea obtained with optical coherence tomography (OCT) of an eye with acute submacular hemorrhage associated with exudative age-related macular degeneration. Using an acute OCT image, three measurements were made in the fovea, including the thickness of the neurosensory retina, thickness of the submacular hemorrhage, and total foveal thickness.

b A cross-sectional image of the fovea obtained with OCT after resolution of the submacular hemorrhage. Using the final OCT image, three measurements were made in the fovea, including the thickness of the neurosensory retina, thickness of the subretinal mass and Bruch's membrane, and total foveal thickness

vitreoretinal interface and the elastic fiber layer of Bruch's membrane. These measurements and evaluations were performed by one retinal specialist.

All statistical analyses were performed using StatView version 4.5 (SAS Institute, Cary, NC, USA). All values are expressed as the mean \pm standard deviation. For statistical analysis, VA measured using a Landolt chart was converted to the logarithm of the minimal angle of resolution (logMAR). In the current study, 1 optic disc area is equal to 2.54 mm² based on an optic disc diameter of 1.8 mm [29]. Bivariate relationships were analyzed using Pearson's correlation coefficient. *P* values <0.05 were considered statistically significant.

Results

In the current study, 31 eyes of 31 patients (21 men and 10 women; age range 66–93 years; mean age 76.8 \pm 7.4 years)

with submacular hemorrhage were examined. Of the 31 eyes, 21 had PCV and 10 had typical AMD. Table 1 shows the characteristics of the patients included in this study. The mean initial VA (logMAR) was 0.69 \pm 0.45. The mean initial area and thickness of the submacular hemorrhage were 6.0 \pm 3.1 disc areas and 315.0 \pm 222.5 μ m, respectively. The follow-up period was 11.3 \pm 7.0 months, ranging from 3 to 28 months.

At the initial examination, each eye exhibited a submacular hemorrhage that affected the fovea. Upon OCT examination, the submacular hemorrhage exhibited intensive or moderate hyperreflectivity depending on its density beneath the neurosensory retina. Of the 31 eyes, the underlying RPE could not be seen at all in 8 because of the shadow cast by the submacular hemorrhage. In addition, the submacular hemorrhage from the CNV or polypoidal lesions seemed to infiltrate the overlying neurosensory retina in many cases. On OCT sections, mild to moderate amorphous hyperreflectivity and/or hyperreflective dots

Table 1 Initial and final conditions of patients with submacular hemorrhage associated with exudative age-related macular degeneration

Age (years)	76.8 ± 7.4
Gender (women/men)	10/21
Type of disease (typical AMD/PCV)	10/21
Initial examination	
Visual acuity (logMAR)	0.69 ± 0.45
Size of submacular hemorrhage (disc areas)	6.0 ± 3.1
Thickness of the neurosensory retina (μm)	194.3 ± 130.3
Thickness of the submacular hemorrhage (μm)	315.0 ± 222.5
Total foveal thickness (μm)	509.2 ± 281.0
Detection of IS/OS under the fovea (complete/incomplete/absent)	3/12/16
Detection of ELM under the fovea (complete/incomplete/absent)	21/2/8
Detection of RPE under the fovea (complete/incomplete/absent)	8/15/8
Duration of symptom (months)	3.7 ± 2.3
Follow-up (months)	11.3 ± 7.0
Final examination	
Visual acuity (logMAR)	0.69 ± 0.47
Cystoid macular edema (%)	11 (35.5 %)
Subfoveal mass (%)	20 (64.5 %)
Thickness of neurosensory retina (μm)	175.4 ± 136.3
Subretinal deposit and Bruch's membrane (μm)	169.5 ± 150.4
Total foveal thickness (μm)	363.7 ± 203.8
Detection of IS/OS under the fovea (complete/incomplete/absent)	3/8/20
Detection of ELM under the fovea (complete/incomplete/absent)	16/5/10

AMD age-related macular degeneration, *PCV* polypoidal choroidal vasculopathy, *logMAR* logarithm of the minimum angle of resolution, *IS/OS* junction between the inner and outer segments of the photoreceptors, *ELM* external limiting membrane, *RPE* retinal pigment epithelium

were seen in the overlying neurosensory retina, especially in the outer aspect, resulting in a lack of IS/OS or ELM lines (Fig. 2). Of the 31 eyes, the foveal IS/OS line could not be observed completely in 28, whereas the foveal ELM line could be observed completely in 21. Intraretinal hyperreflective lesions due to submacular hemorrhage were occasionally observed mainly outside the ELM. In these eyes, the ELM seemed to work as a blocking agent against the hemorrhage (Fig. 2).

Table 2 shows the relationships between the initial VA and other measured values obtained at the initial examination. The etiology of the original disease (typical AMD or PCV) was not correlated with the initial VA ($r = 0.194$, $p = 0.300$). However, the size and thickness of the submacular hemorrhage were both correlated with the initial VA ($r = 0.411$, $p = 0.022$; $r = 0.485$, $p = 0.0057$). In addition, detection of the RPE beneath the fovea, which seemed to reflect the density of the submacular hemorrhage, was correlated with the initial VA ($r = 0.479$, $p = 0.0064$). While the thickness of the neurosensory retina was not correlated with the initial VA ($r = 0.203$, $p = 0.274$), detection of the foveal ELM was correlated with initial VA ($r = 0.423$, $p = 0.018$).

At the final examination, all eyes exhibited a complete absorption of the submacular hemorrhage, and the mean final VA was 0.69 ± 0.47 (logMAR). Cystoid macular edema was observed in 11 eyes. Twenty eyes exhibited a

subretinal mass, the mean thickness of which, including the Bruch's membrane, was 169.5 ± 150.4 μm. In addition, submacular hemorrhages caused substantial damage to the overlying outer retina. The IS/OS were completely detected in only 3 and the ELM lines in 16 eyes.

Table 3 shows the relationships between the final VA and other measured values obtained at the final examination. The etiology of the original disease (typical AMD or PCV) was not correlated with the final VA ($r = 0.249$, $p = 0.176$). However, cystoid macular edema and subfoveal mass were correlated with poor final VA ($r = 0.355$, $p = 0.050$; $r = 0.477$, $p = 0.0067$). The total retinal thickness and the thickness of the subfoveal mass at the final examination were correlated with poor final VA ($r = 0.607$, $p = 0.0003$; $r = 0.489$, $p = 0.0052$). In addition, the integrity of the foveal photoreceptor layer contributed to foveal function. Detection of the IS/OS and ELM lines beneath the fovea were both strongly correlated with good final VA ($r = 0.574$, $p = 0.0007$; $r = 0.756$, $p < 0.0001$).

Table 4 shows the relationships between the final VA and measured values obtained at the initial examination. The final VA was 0.86 ± 0.39 with typical AMD and 0.61 ± 0.49 with PCV ($p = 0.176$). The etiology of the original disease was not correlated with the final VA ($r = 0.249$, $p = 0.176$). Although the submacular hemorrhage thickness and density were weakly correlated with the

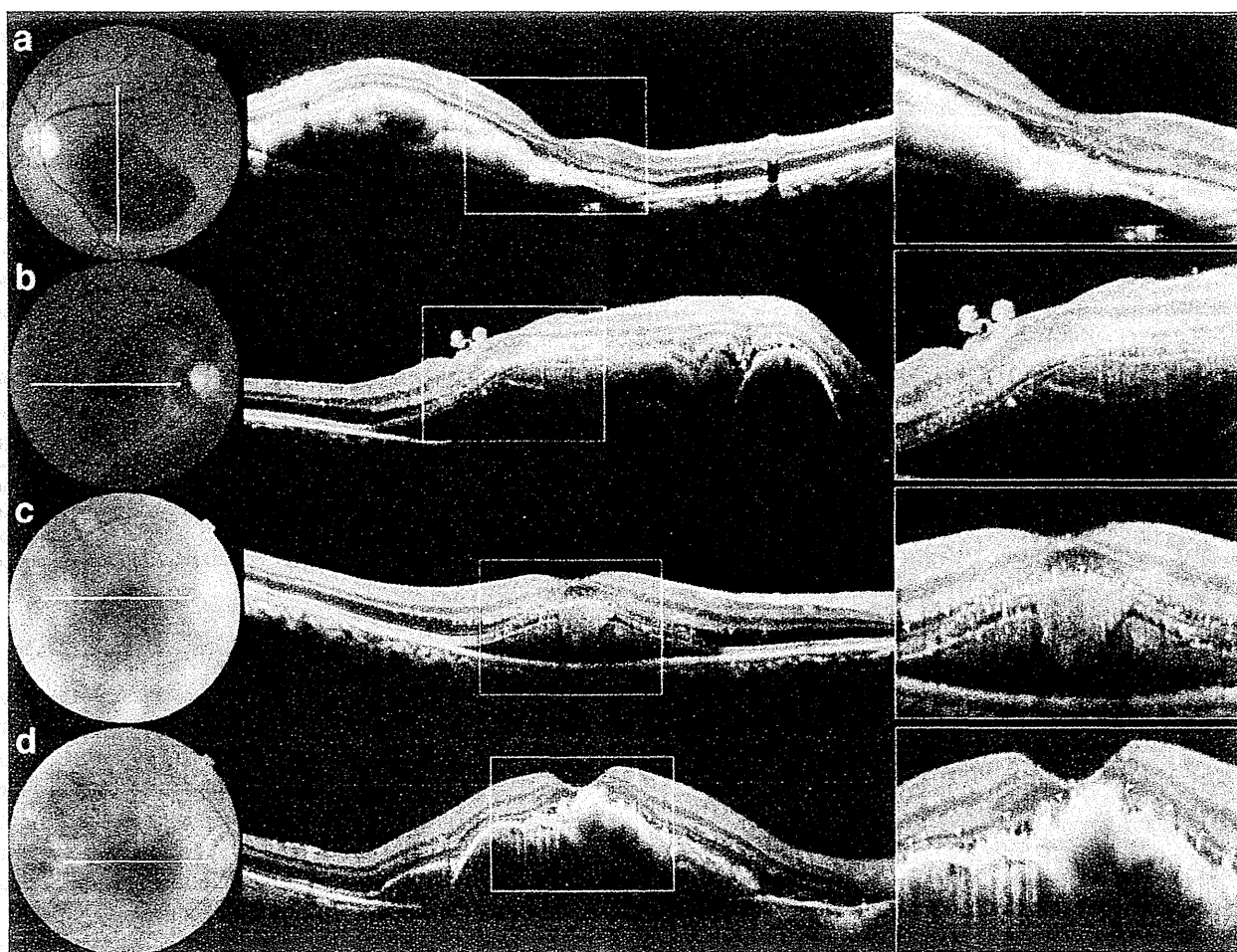


Fig. 2 Cross-sectional images obtained by optical coherence tomography (OCT) in eyes with acute submacular hemorrhage associated with exudative age-related macular degeneration. Each OCT section (middle in each case) was made along an arrow shown in the fundus photographs (left in each case). Magnified OCT images (right in each case) were made from the delimited boxes in OCT sections. **a** On the OCT section, the submacular hemorrhage shows intensive hyperreflectivity beneath the neurosensory retina. Within the outer aspect of the neurosensory retina, several hyperreflective dots are seen. The structure of the neurosensory retina seems to be relatively well preserved. Visual acuity was 0.5 **b** On the OCT section, submacular hemorrhage

shows moderate hyperreflectivity. Amorphous hyperreflectivity and numerous hyperreflective dots are seen within the neurosensory retina. Visual acuity was 0.09 **c** On the OCT section, submacular hemorrhage shows moderate hyperreflectivity. Amorphous hyperreflectivity and numerous hyperreflective dots are seen in neurosensory retina, especially in the outer aspect. Under the fovea, infiltration of the hemorrhage into the neurosensory retina seems to be blocked by the external limiting membrane (arrowheads). Visual acuity was 0.4 **d** On the OCT section, submacular hemorrhage shows intensive hyperreflectivity. Under the fovea, the hemorrhage seems to invade the neurosensory retina beyond the external limiting membrane (arrowheads). Visual acuity was 0.08

final VA ($r = 0.258$, $p = 0.161$; $r = 0.281$, $p = 0.126$), the size of the submacular hemorrhage was not ($r = 0.111$, $p = 0.554$). However, the initial integrity of the foveal photoreceptor layer was correlated with visual prognosis. While the initial detection of the ELM beneath the fovea was not correlated with final VA ($r = 0.063$, $p = 0.736$), the initial detection of the IS/OS beneath the fovea was correlated with good final VA ($r = 0.375$, $p = 0.038$) (Figs. 3, 4). In the subgroup analysis, eyes with typical AMD and PCV exhibited a similar tendency, respectively, although the correlations were not statistically significant

($r = 0.566$, $p = 0.088$ with AMD; $r = 0.331$, $p = 0.142$ with PCV); this is possibly due to the small number of eyes in each group.

Discussion

Acute serous retinal detachment associated with central serous chorioretinopathy does not usually cause a severe decrease in VA, even if there is subretinal fluid under the fovea [30]. However, submacular hemorrhage often

Table 2 Association of initial visual acuity with other measurements obtained at the initial examination

	<i>r</i>	<i>p</i> value
Age (years)	0.018	0.922
Type of disease (typical AMD/PCV)	0.194	0.300
Size of submacular hemorrhage (disc areas)	0.411	0.022
Thickness of the neurosensory retina (μm)	0.203	0.274
Thickness of the submacular hemorrhage (μm)	0.485	0.0057
Total foveal thickness (μm)	0.478	0.0065
Detection of IS/OS under the fovea	0.272	0.139
Detection of ELM under the fovea	0.423	0.018
Detection of RPE under the fovea	0.479	0.0064

AMD age-related macular degeneration, *PCV* polypoidal choroidal vasculopathy, *logMAR* logarithm of the minimum angle of resolution, *IS/OS* junction between the inner and outer segments of the photoreceptors, *ELM* external limiting membrane, *RPE* retinal pigment epithelium

Table 3 Association of final visual acuity with other measurements obtained at the final examination

	<i>r</i>	<i>p</i> value
Age (years)	0.244	0.186
Type of disease (typical AMD/PCV)	0.249	0.176
Duration of symptom (months)	0.182	0.327
Cystoid macular edema	0.355	0.050
Subfoveal mass	0.477	0.0067
Thickness of the neurosensory retina (μm)	0.277	0.132
Thickness of subretinal mass and Bruch's membrane (μm)	0.489	0.0052
Total foveal thickness (μm)	0.607	0.0003
Detection of IS/OS under the fovea (%)	0.574	0.0007
Detection of ELM under the fovea (%)	0.756	<0.0001

AMD age-related macular degeneration, *PCV* polypoidal choroidal vasculopathy, *logMAR* logarithm of the minimum angle of resolution, *RPE* retinal pigment epithelium, *IS/OS* the junction between inner and outer segments of the photoreceptors, *ELM* external limiting membrane

accompanies acute severe visual loss immediately after onset [2]. Histologic reports show that submacular hemorrhage causes severe damage to the outer retina [16, 17], and experimental reports suggest mechanisms by which chronic damage to the photoreceptor layer occurs [18, 19]. However, in addition to chronic effects, bleeding within the subretinal space can exert immediate effects on the neurosensory retina, thereby causing acute visual dysfunction [15].

The initial OCT sections of our patients revealed that the submacular hemorrhage exhibited hyperreflectivity beneath the neurosensory retina. In addition, the overlying neurosensory retina often exhibited hyperreflective lesions. In

Table 4 Association of final visual acuity with measurements obtained at the initial examination

	<i>r</i>	<i>p</i> value
Age (years)	0.244	0.186
Type of disease (typical AMD/PCV)	0.249	0.176
Size of subretinal hemorrhage (disc areas)	0.111	0.554
Visual acuity (logMAR)	0.295	0.107
Thickness of the neurosensory retina (μm)	0.100	0.594
Thickness of the submacular hemorrhage (μm)	0.268	0.145
Total foveal thickness (μm)	0.258	0.161
Detection of IS/OS under the fovea	0.375	0.038
Detection of ELM under the fovea	0.063	0.736
Detection of RPE under the fovea	0.281	0.126

AMD age-related macular degeneration, *PCV* polypoidal choroidal vasculopathy, *logMAR* logarithm of the minimum angle of resolution, *IS/OS* junction between the inner and outer segments of the photoreceptors, *ELM* external limiting membrane, *RPE* retinal pigment epithelium

the current study, amorphous hyperreflectivity of various intensities and hyperreflective dots were observed in the outer aspect of the overlying neurosensory retina. Immediately after bleeding within the subretinal space, erythrocytes, macrophages, and fibrin can migrate into the outer retina and may destroy the integrity of the photoreceptor layer [31]. Ooto et al. [32] report the relationship between VA and fibrin infiltration within the neurosensory retina in eyes with PCV. In addition, Coscas et al. [27] state that bright hyperreflective spots and hyperreflective material within the neurosensory retina could be derived from an inflammatory reaction, and they indicate the activity of exudative AMD. Based on previous reports [32, 33], our findings related to the neurosensory retina may be associated with acute dysfunction of the macula, which results in an acute loss of central vision.

In the current study, while the IS/OS line beneath the fovea was detected completely at the initial visit in only 3 eyes, complete detection of the ELM line under the fovea was achieved in 21 eyes. In fact, the ELM line was frequently preserved even in the eyes with a thick submacular hemorrhage. On OCT sections, the ELM line sometimes appeared to act as a blocking agent against the advancement of hemorrhage into the retina after the hemorrhage had already infiltrated the inner and outer segments. Our OCT findings can be explained according to the theory on the mechanisms of fluid movement proposed by Marmor [34]. He reports that the ELM, which consists of the zonula adherens between Müller cells and photoreceptors at the base of the outer segments, works as a weak anatomic barrier to the movement of large protein molecules in the retina.

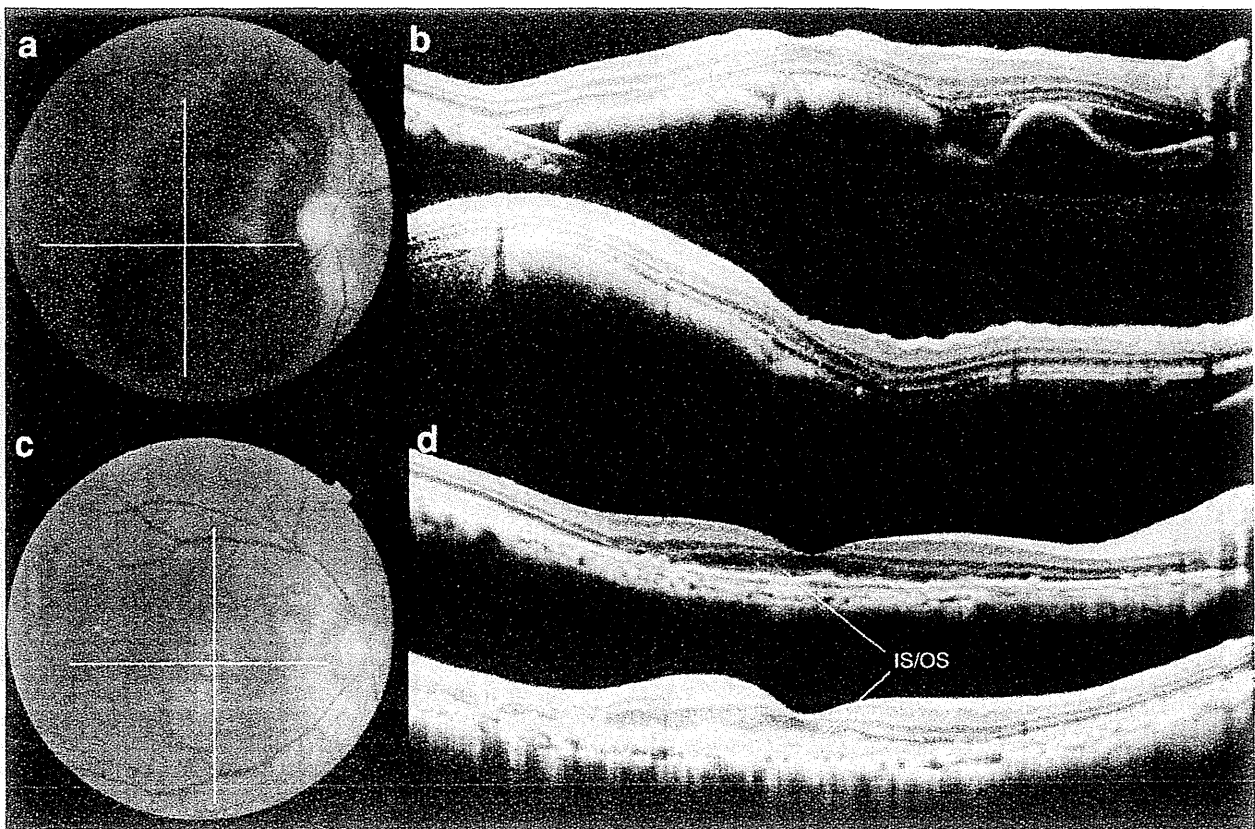


Fig. 3 Good recovery of vision in eyes with submacular hemorrhage associated with polypoidal choroidal vasculopathy. **a** A 66-year-old woman with a sudden decrease of vision in the right eye (0.2 OD), at which time she had a large submacular hemorrhage. **b** Initial horizontal (*upper*) and vertical (*lower*) optical coherence tomographic images along the *white arrows* shown in the fundus photograph show intensive hyperreflectivity of the submacular hemorrhage beneath the neurosensory retina. Several *hyperreflective dots* are seen in the

neurosensory retina; but the structure of the neurosensory retina seems to be well preserved. The line of the junction between inner and outer segments of the photoreceptors (IS/OS) is seen under the fovea. **c** At 12 months, the submacular hemorrhage was completely absorbed. **d** Horizontal (*upper*) and vertical (*lower*) optical coherence tomographic images along the *white arrows* show good preservation of the neurosensory retina. The IS/OS line is seen under the fovea and visual acuity has improved to 0.8 OD

Previous reports on the natural history of submacular hemorrhage suggest that exudative AMD is associated with poor visual prognosis, especially when subretinal fibrosis is observed after the resolution of the hemorrhage [3, 5]. In the current study, 64.5 % of the eyes exhibited a subfoveal mass at the final examination; the thickness of this mass was strongly correlated with the final VA. In addition, recent studies with OCT show that the integrity of the foveal photoreceptor layer—especially its outer aspect—is necessary if good visual function is to be achieved [35]. A few years ago, Hayashi et al. [36] reported the association between intact foveal IS/OS and good VA after the successful treatment of exudative AMD with photodynamic therapy. Oishi et al. [37] suggest that foveal ELM is associated with final VA in exudative AMD treated with photodynamic therapy. Consistent with these reports, our study shows that after complete resolution of the

submacular hemorrhage, complete detection of the IS/OS and ELM lines are correlated with final VA.

So far, various factors have been suggested to be associated with visual prognosis, including the initial VA [4, 5], size or thickness of the submacular hemorrhage [3, 4, 6], and etiology of the original disease [3, 5]. As mentioned above, visual prognosis was poor in the eyes with submacular hemorrhage resulting from exudative AMD [3], especially in the eyes with subretinal CNV [5]. While the relationship between the size of the hemorrhage and the final VA varies, most previous studies indicate that the initial thickness of the hemorrhage is associated with visual prognosis [3, 4, 6]. However, in those studies, the thickness of the submacular hemorrhage was evaluated as the elevation of the neurosensory retina detected by stereoscopic photography; no quantitative evaluations were performed. In the current study, the initial size of the hemorrhage was

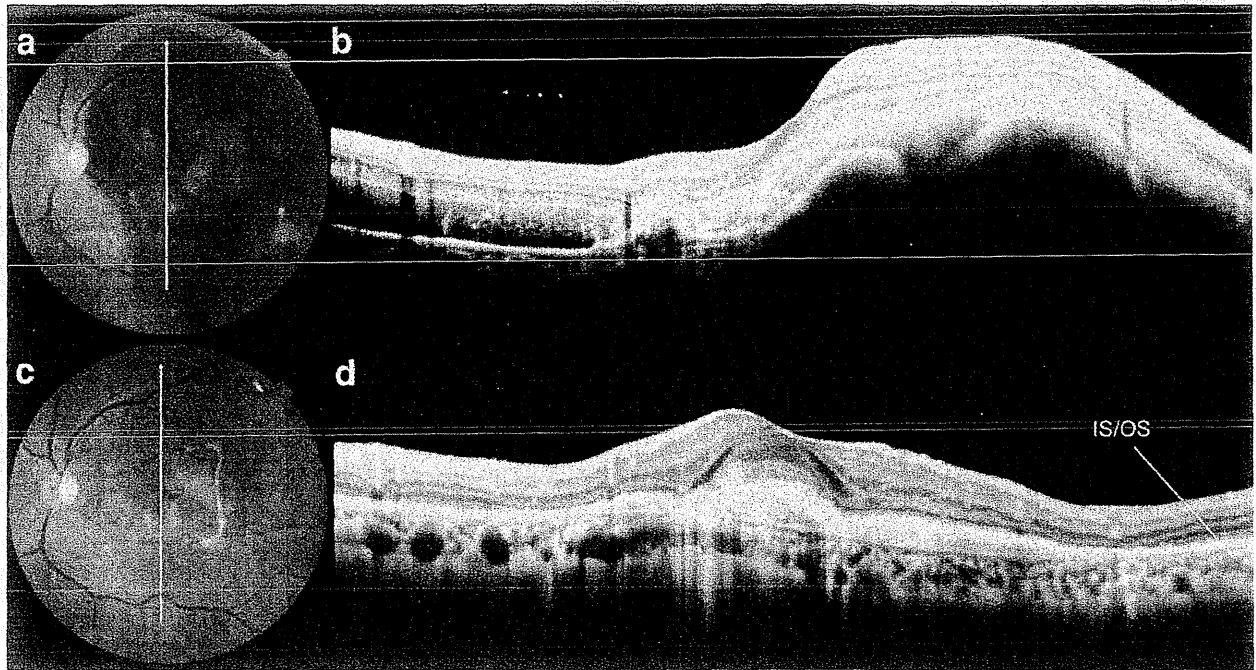


Fig. 4 Poor recovery of vision in eyes with submacular hemorrhage associated with polypoidal choroidal vasculopathy. **a** A 67-year-old man with a sudden decrease of vision in the left eye (0.4 OS), at which time he was noted to have a massive submacular hemorrhage. **b** Initial optical coherence tomographic image along the *white arrows* shown in the fundus photograph reveals intensive hyperreflectivity of the submacular hemorrhage beneath the neurosensory retina.

Amorphous *hyperreflectivity* and *hyperreflective dots* are seen in overlying neurosensory retina. The line of the junction between inner and outer segments of the photoreceptors (IS/OS) is not detectable under the fovea. **c** At 14 months, the submacular hemorrhage has been absorbed completely. **d** Optical coherence tomographic image along the *white arrows* shows a thick subfoveal deposit. The IS/OS line is seen under the fovea, but visual acuity remained 0.3 OS

not correlated with the final VA. However, the thickness and density of the hemorrhage were both weakly correlated with final VA.

It is certain that the integrity of the outer photoreceptor layer in the fovea contributes to VA [35–38]. In the current study, initial detection of the ELM line beneath the fovea was correlated with the initial but not final VA. While the foveal ELM was initially detected in 21 eyes, complete detection was achieved at the final examination in only 16 eyes. The chronic harmful effects of submacular hemorrhage include damage to the foveal photoreceptor layer, which results in a decline in VA [16]. However, the initial detection of the foveal IS/OS line was correlated with visual prognosis. The inner and outer segments of the photoreceptor layer located outside the ELM, which are assumed to function as a blockade against hemorrhage infiltration [34], are vulnerable to acute submacular hemorrhage [19, 39]. The foveal IS/OS line was detected completely at the initial visit in only three of our patients. In such eyes, acute effects on the neurosensory retina may be minimal, resulting in good visual prognosis.

In experimental studies with animal models, the suggested mechanisms of damage to the photoreceptor layer

include clot retraction [19], iron toxicity [20, 21], and blockage of nutrient diffusion by iron [18]. Submacular hemorrhage may block the exchange of nutrients and metabolites between the neurosensory retina and RPE [18]. The chief toxic agent released from submacular hemorrhage is thought to be iron in the form of ferritin [2]. In an experimental model of submacular hemorrhage, increased iron levels in the outer segments of the photoreceptor layer are thought to exert a toxic effect on the outer segment lipids via oxidative stress [39]. In addition, an experimental study by Toth et al. [19] shows that fibrin produced by submacular hemorrhage interdigitates with the outer photoreceptor segments and subsequently tears the sheet of both the inner and the outer photoreceptor segments. In the current study, the detection of the foveal IS/OS line at the initial examination was correlated with good final VA. In these eyes, the lack of fibrin interdigitation and the low level of iron toxicity could explain the good visual prognosis.

The limitations of the current study include its retrospective nature, various treatment regimens used, and small sample size. Treatment modality may have some influence on the visual prognosis [40, 41]. Several factors may be mutually related, but the number of eyes was too small to

perform multiple univariate testing. In addition, while no eyes showed residual submacular hemorrhage at the final visits, the follow-up period of some eyes was too short to discuss the visual prognosis [42]. Another limitation is that the current study involved eyes with typical AMD and PCV. However, despite these limitations, our findings suggest that submacular hemorrhages often infiltrate the overlying neurosensory retina, harming the structure of the outer retina. As a hallmark of the integrity of the foveal photoreceptor layer, the initial detection of the IS/OS just beneath the fovea may be associated with good visual outcomes. Previous studies report a better visual prognosis for PCV [43]. We analyzed the subgroups of typical AMD and PCV to confirm the correlation between the initial detection of the foveal IS/OS and final VA. Each group exhibited a similar tendency, but the correlation was not statistically significant, possibly because of the small number of eyes in each group. Further prospective studies are necessary to confirm the correlations reported in the current study.

References

- Woo JJ, Lou PL, Ryan EA, Kroll AJ Surgical treatment of submacular hemorrhage in age-related macular degeneration. *Int Ophthalmol Clin*. 2004;44:43–50.
- Steel DH, Sandhu SS. Submacular haemorrhages associated with neovascular age-related macular degeneration. *Br J Ophthalmol*. 2011;95:1051–7.
- Bennett SR, Folk JC, Blodi CF, Klugman M. Factors prognostic of visual outcome in patients with subretinal hemorrhage. *Am J Ophthalmol*. 1990;109:33–7.
- Avery RL, Fekrat S, Hawkins BS, Bressler NM. Natural history of subfoveal subretinal hemorrhage in age-related macular degeneration. *Retina*. 1996;16:183–9.
- Berrocal MH, Lewis ML, Flynn HW Jr. Variations in the clinical course of submacular hemorrhage. *Am J Ophthalmol*. 1996;122:486–93.
- Scupola A, Coscas G, Soubrane G, Balestrazzi E. Natural history of macular subretinal hemorrhage in age-related macular degeneration. *Ophthalmologica*. 1999;213:97–102.
- de Juan E, Jr Machemer R. Vitreous surgery for hemorrhagic and fibrous complications of age-related macular degeneration. *Am J Ophthalmol*. 1988;105:25–9.
- Wade EC, Flynn HW Jr, Olsen KR, Blumenkranz MS, Nicholson DH. Subretinal hemorrhage management by pars plana vitrectomy and internal drainage. *Arch Ophthalmol*. 1990;108:973–8.
- Stifter E, Michels S, Prager F, Georgopoulos M, Polak K, Hirn C, et al. Intravitreal bevacizumab therapy for neovascular age-related macular degeneration with large submacular hemorrhage. *Am J Ophthalmol*. 2007;144:886–92.
- Fine HF, Iranmanesh R, Del Priore LV, Barile GR, Chang LK, Chang S, et al. Surgical outcomes after massive subretinal hemorrhage secondary to age-related macular degeneration. *Retina*. 2010;30:1588–94.
- Ohji M, Saito Y, Hayashi A, Lewis JM, Tano Y. Pneumatic displacement of subretinal hemorrhage without tissue plasminogen activator. *Arch Ophthalmol*. 1998;116:1326–32.
- Kamei M, Tano Y, Maeno T, Ikuno Y, Mitsuda H, Yuasa T. Surgical removal of submacular hemorrhage using tissue plasminogen activator and perfluorocarbon liquid. *Am J Ophthalmol*. 1996;121:267–75.
- Lim JJ, Drews-Botsch C, Sternberg P Jr, Capone A Jr, Aaberg TM Sr. Submacular hemorrhage removal. *Ophthalmology*. 1995;102:1393–9.
- Hassan AS, Johnson MW, Schneiderman TE, Regillo CD, Tornambe PE, Poliner LS, et al. Management of submacular hemorrhage with intravitreal tissue plasminogen activator injection and pneumatic displacement. *Ophthalmology*. 1999;106:1900–6.
- Tsujikawa A, Sakamoto A, Ota M, Oh H, Miyamoto K, Kita M, et al. Retinal structural changes associated with retinal arterial macroaneurysm examined with optical coherence tomography. *Retina*. 2009;29:782–92.
- Green WR, Key SN 3rd. Senile macular degeneration: a histopathologic study. *Trans Am Ophthalmol Soc*. 1977;75:180–254.
- Reynders S, Lafaut BA, Aisenbrey S, Broecke CV, Lucke K, Walter P, et al. Clinicopathologic correlation in hemorrhagic age-related macular degeneration. *Graefes Arch Clin Exp Ophthalmol*. 2002;240:279–85.
- Glatt H, Machemer R. Experimental subretinal hemorrhage in rabbits. *Am J Ophthalmol*. 1982;94:762–73.
- Toth CA, Morse LS, Hjelmeland LM, Landers MB 3rd. Fibrin directs early retinal damage after experimental subretinal hemorrhage. *Arch Ophthalmol*. 1991;109:723–9.
- Koshihbu A. Ultrastructural studies on absorption of an experimentally produced subretinal hemorrhage. III. Absorption of erythrocyte break down products and retinal hemosiderosis at the late stage. *Nippon Ganka Gakkai Zasshi*. 1979;83:386–400. (in Japanese).
- el Baba F, Jarrett WH 2nd, Harbin TS Jr, Fine SL, Michels RG, Schachat AP, et al. Massive hemorrhage complicating age-related macular degeneration. Clinicopathologic correlation and role of anticoagulants. *Ophthalmology*. 1986;93:1581–92.
- Drexler W, Sattmann H, Hermann B, Ko TH, Stur M, Unterhuber A, et al. Enhanced visualization of macular pathology with the use of ultrahigh-resolution optical coherence tomography. *Arch Ophthalmol*. 2003;121:695–706.
- Ko TH, Fujimoto JG, Schuman JS, Paunescu LA, Kowalevicz AM, Hartl I, et al. Comparison of ultrahigh- and standard-resolution optical coherence tomography for imaging macular pathology. *Ophthalmology*. 2005;112:1922–35.
- Wojtkowski M, Bajraszewski T, Gorczynska I, Targowski P, Kowalczyk A, Wasilewski W, et al. Ophthalmic imaging by spectral optical coherence tomography. *Am J Ophthalmol*. 2004;138:412–9.
- Chen TC, Cense B, Pierce MC, Nassif N, Park BH, Yun SH, et al. Spectral domain optical coherence tomography. ultra-high speed, ultra-high resolution ophthalmic imaging. *Arch Ophthalmol*. 2005;123:1715–20.
- Coscas F, Coscas G, Souied E, Tick S, Soubrane G. Optical coherence tomography identification of occult choroidal neovascularization in age-related macular degeneration. *Am J Ophthalmol*. 2007;144:592–9.
- Coscas G, Coscas F, Vismara S, Zourdam A, Li Calzi CI. Clinical features and natural history of AMD. In: Coscas G, Coscas F, Vismara S, Zourdam A, Li Calzi CI, editors. *Optical coherence tomography in age-related macular degeneration*. Heidelberg: Springer, 2009. p. 171–274.
- Mavroufides EC, Villate N, Rosenfeld PJ, Puliafito CA. Age-related macular degeneration. 2nd ed. In: Schuman JS, Puliafito CA, Fujimoto JG, editors. *Optical coherence tomography Thorofare*. Slack, 2004. p. 243–344.
- Rosenfeld PJ, Brown DM, Heier JS, Boyer DS, Kaiser PK, Chung CY, et al. Ranibizumab for neovascular age-related macular degeneration. *N Engl J Med*. 2006;355:1419–31.

30. Spaide RF. Central serous chorioretinopathy. In: Holz FG, Spaide RF, editors. *Medical retina*. Berlin: Springer; 2004. p. 77–93.
31. Lincoff H, Madjarov B, Lincoff N, Movshovich A, Saxena S, Coleman DJ, et al. Pathogenesis of the vitreous cloud emanating from subretinal hemorrhage. *Arch Ophthalmol*. 2003;121:91–6.
32. Ooto S, Tsujikawa A, Mori S, Tamura H, Yamashiro K, Otani A, et al. Retinal microstructural abnormalities in central serous chorioretinopathy and polypoidal choroidal vasculopathy. *Retina*. 2011;31:527–34.
33. Coscas G, Coscas F, Vismara S, Zourdan A, Li Calzi CI. OCT interpretation. In: Coscas G, Coscas F, Vismara S, Zourdan A, Li Calzi CI, editors. *Optical coherence tomography in age-related macular degeneration*. Heidelberg: Springer; 2009. p. 97–170.
34. Marmor MF. Mechanisms of fluid accumulation in retinal edema. *Doc Ophthalmol*. 1999;97:239–49.
35. Costa RA, Calucci D, Skaf M, Cardillo JA, Castro JC, Melo LA Jr, et al. Optical coherence tomography 3: automatic delineation of the outer neural retinal boundary and its influence on retinal thickness measurements. *Invest Ophthalmol Vis Sci*. 2004;45:2399–406.
36. Hayashi H, Yamashiro K, Tsujikawa A, Ota M, Otani A, Yoshimura N. Association between foveal photoreceptor integrity and visual outcome in neovascular age-related macular degeneration. *Am J Ophthalmol*. 2009;148:83–9.
37. Oishi A, Hata M, Shimozono M, Mandai M, Nishida A, Kurimoto Y. The significance of external limiting membrane status for visual acuity in age-related macular degeneration. *Am J Ophthalmol*. 2010;150:27–32.
38. Sandberg MA, Brockhurst RJ, Gaudio AR, Berson EL. The association between visual acuity and central retinal thickness in retinitis pigmentosa. *Invest Ophthalmol Vis Sci*. 2005;46:3349–54.
39. Bhisitkul RB, Winn BJ, Lee OT, Wong J, Pereira Dde S, Porco TC, et al. Neuroprotective effect of intravitreal tramcinolone acetamide against photoreceptor apoptosis in a rabbit model of subretinal hemorrhage. *Invest Ophthalmol Vis Sci*. 2008;49:4071–7.
40. Kim KS, Lee WK. Bevacizumab for serous changes originating from a persistent branching vascular network following photodynamic therapy for polypoidal choroidal vasculopathy. *Jpn J Ophthalmol*. 2011;55:370–7.
41. Nakata I, Yamashiro K, Nakanishi H, Tsujikawa A, Otani A, Yoshimura N. VEGF gene polymorphism and response to intravitreal bevacizumab and triple therapy in age-related macular degeneration. *Jpn J Ophthalmol*. 2011;55:435–43.
42. Akaza E, Yuzawa M, Mori R. Three-year follow-up results of photodynamic therapy for polypoidal choroidal vasculopathy. *Jpn J Ophthalmol*. 2011;55:39–44.
43. Sho K, Takahashi K, Yamada H, Wada M, Nagai Y, Otsuji T, et al. Polypoidal choroidal vasculopathy: incidence, demographic features, and clinical characteristics. *Arch Ophthalmol*. 2003;121:1392–6.

